RSC Advances

ROYAL SOCIETY OF CHEMISTRY

www.rsc.org/advances

Cite this: DOI: 10.1039/c0xx00000x

www.rsc.org/xxxxxx

ARTICLE TYPE

Enhanced performance of Fe^{3+} detection via fluorescence resonance energy transfer between carbon quantum dots and Rhodamine B

Shengliang Hu, *[a,b‡]Qing Zhao,[b‡] Qing Chang, *[b] Jinlong Yang,[b,c] and Jun Liu[a]

Received (in XXX, XXX) Xth XXXXXXXXX 200X, Accepted Xth XXXXXXXXX 200X

DOI: 10.1039/b000000x

Carbon quantum dots (CQDs) were prepared by a facile hydrothermal method and emited a broad fluorescence covering the whole blue and green light wavelength scope. Because their emission spectra overlaped with the absoprtion spectrum of Rhodamine B (RhB) molecules, fluorescent resonance energy transfer (FRET) phenomenon between CQDs as energy donors and RhB as energy acceptors was observed when CQDs mix with RhB in solution. To obtain the optimal FRET efficiency, the concentrations of CQDs and RhB should be ajusted to 0.559 mg mL^{-1} and 1.25 μM, respectively, at pH=6.2. None of metal ions except for Fe^{3+} ions hindered this FRET process as well as deactivated electronic excitation energy of RhB molecules through migration, resulting in enhancement of fluorescence quenching rates. Therefore, the developed system allowed enhancing selectivity and sensitivity of Fe^{3+} detection via FRET effects, and could be used for accurate measurements of time-dependent conformational change and monitoring corrosion process of iron materials over an extended period.

1. Introduction

Fluorescence resonance energy transfer (FRET) is a process in which involves the non-radiative transfer of excitation energy from an excited donor to an acceptor.[1-3] It has been employed on enhancing selectivity and sensitivity of fluorescence probe. At present, traditional quantum dots (such as CdTe and CdSe) were generally used as the excited state energy donor in FRET system.[4-9] However, they have a limitation because of containing toxic elements. Carbon quantum dots (CQDs) as a new kind of fluorescent probe has exhibited many advantages, including of photoluminescence tunability, long fluorescence lifetime and high photostability without incurring the burden of intrinsic toxicity or elemental scarcity.[10-19] Therefore, many efforts were made to develop CQDs application in the detection system. Several successful examples had been reported, for instance, some metal ions (such as Cu^{2+}, Hg^{2+} and Ag^{+}) were recognized through fluorescence changes of CQDs.[20-25]However, few reported that CQDs was acted as a component of FRET system to recognize metal ions.

Rhodamine B (RhB) that belongs to the group of xanthene dyes that are commonly used in FRET system as the excited state energy acceptor because of its many advantages, such as good solubility, excellent photostability, high extinction coefficient and fluorescence quantum yields.[26,27] It had been utilized in FRET system to detect DNA, metal ions, small molecules, and other analytes.[4,5,28,29] In the present work, the FRET effect between CQDs and RhB was observed and used for fluorescence probe to detect Fe^{3+} ions. Significantly, the FRET system of CQDs and RhB (RhB@CQDs) showed the higher selectivity and sensitivity towards Fe^{3+} ions compared to RhB and CQDs, respectively.

2. Experiments

Materials and Apparatus

Ethylene glycol and Rhodamine B were purchased from Aladdin (Shanghai, China). A variety of cations were introduced by soluble metal salts, such as $Fe(NO_3)_3$, $Al(NO_3)_3$, $MnCl_2$, $Pb(NO_3)_2$, $NiCl_2$, $CaCl_2$, $CuCl_2$, $ZnCl_2$, $HgCl_2$, $Mg(NO_3)_2$, $Fe(SO_4)_2$, Na_2CO_3, KCl, $Ba(NO_3)_2$ and $CdCl_2$. Absorption and FL emission was measured by Shimadzu UV-2550 UV/Vis spectrometer and Hitachi F4500 fluorescence spectrophotometer, respectively. Transmission electron microscopy (TEM) and high-resolution TEM (HRTEM) images were obtained using a FEI Tecnai G2 F20 microscope with a field-emission gun operating at 200 kV. The infrared spectra were obtained on a Thermo Nicolet 360 FT-IR spectrophotometer.

Preparation of RhB@CQDs

The CQDs were prepared by hydrothermal treatment of ethylene glycol as our reported previously.[30] Briefly, 25 mL of ethylene glycol was transferred into a 50 mL Teflon equipped stainless steel autoclave and then placed in a drying oven at 200 °C for 5 h. After cooling to room temperature, the transparent solution contained CQDs were obtained. Next, it was mixed with 125 μL of RhB (0.5 mM). After stirring for above 2 h at room temperature, the complex of RhB@CQDs was finally obtained. The samples of pH were adjusted by adding HCl and NaOH.

3. Results

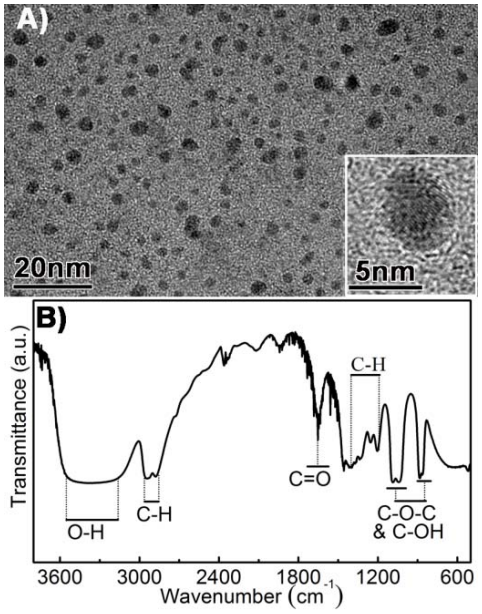

Figure 1A) TEM and HRTEM images of CQDs; B) FTIR spectrum of CQDs

As shown in Figure 1A, TEM image of CQDs reveals that they are dispersed uniformly with their size of several nanometers. The typical HRTEM image shows lattice finges with interplanar spacings similar to graphitic structure. FTIR spectrum (Figure 1B) further suggests that some O-contained groups including of C=O, C-O-C and OH groups are present in the CQDs. Such surface groups impart CQDs with excellent water solubility and the suitability for subsequent functionalization with various organic, inorganic species via covalent or noncovalent bonds.

FRET generally requires a nonzero integral of the spectral overlap between donor emission and acceptor absorption.[1-3] Therefore, the normalized fluorescence (FL) emission spectrum of CQDs and absorption spectrum of RhB molecules are shown in Figure 2 A.It can be seen that the spectral overlap is present in the shadow area. Figure 2B shows the FL emission comparisons between CQDs, RhB and RhB@CQDs. RhB@CQDs exhibits two FL peaks at 427 and 581 nm, respectively. FL peak at 427 nm from RhB@CQDs becomes weaker than that from only CQDs while FL peak at 581 nm is significantly stronger than that from only RhB molecules at the same excitation wavelength. This suggests that the excited CQDs are transferred energy into RhB molecules, i.e. FRET occurs. However, the FL emission obtained at the excitation wavelength of 365 nm quenched significantly when Fe^{3+} ions were added into the system of RhB@CQDs (Figure 2C). Figure 2D gives the FL emission behaviors of RhB@CQDs excited at the wavelength of 554 nm, which is the maximum absorption peak of RhB molecules, under the conditions of the absence and presence of Fe^{3+} ions. It is noted that CQDs hardly emit at the excitation wavelength of 554 nm and thus the emission obtained by 554 nm excitation is attributed to RhB molecules. According to Figure 2D, Fe^{3+} ions also quenched FL emission of RhB molecules. However, the different quenching degrees were obtained at the same content of Fe^{3+} ions when both 365 and 554 nm excitation wavelength were employed, respectively (Figure 2C and D). Furthermore, Fe^{3+} ions also made FL emission peak at 581 nm a little red-shift no mater which excitation wavelengths are employed.

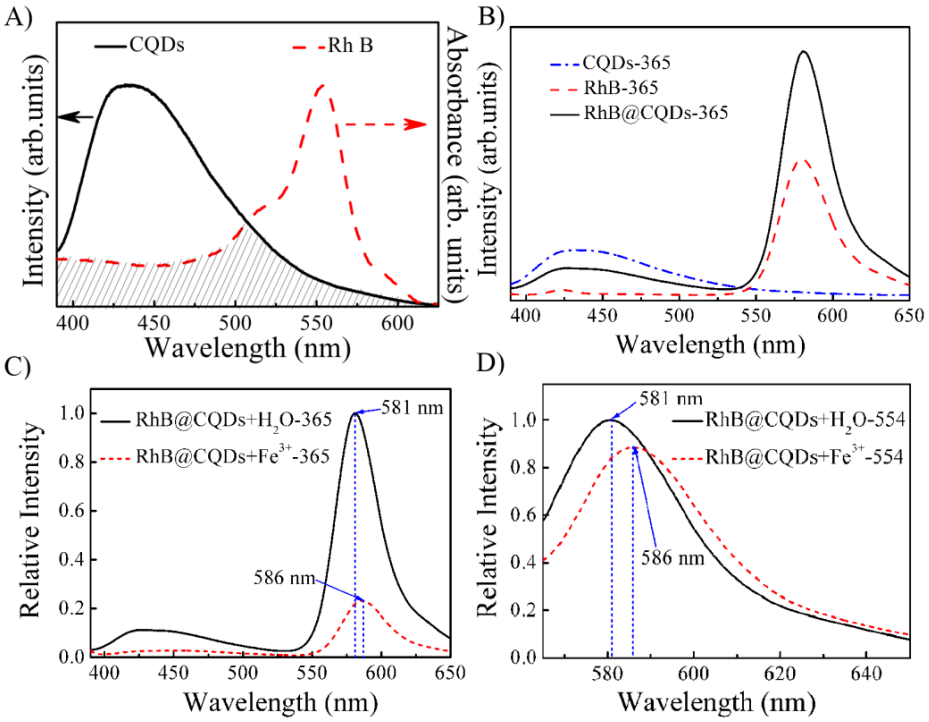

Figure 2 A) The normalized FL emission spectrum of CQDs and absorption spectra of RhB; B) The FL emission spectra of CQDs, RhB and RhB@CQDs at the excitation wavelength of 365 nm; C) and D) The FL emission spectra of RhB@CQDs in the absence and presence of 500 μM Fe^{3+} at the excitation wavelength of 365 and 554 nm, respectively.

Figure 3 shows the comparisons of emission quenching rates of the FL emission peaks at 427 and 581 nm between CQDs, RhB

and RhB@CQDs under the same content of Fe^{3+} ions. The emission quenching rate of RhB@CQDs is 2.5 times higher than that of CQDs and RhB, respectively, suggesting that RhB@CQDs has a high efficiency to detect Fe^{3+} ions.

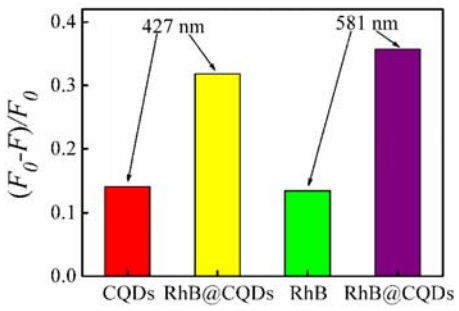

Figure 3 The quenching rate comparisons of FL emission peaks at 427 and 581 nm, respectively, between CQDs, RhB and RhB@CQDs in the presence of 500 μM Fe^{3+} ions. Here, F_0 and F are the FL emission intensities of CQDs, RhB and RhB@CQDs without and with Fe^{3+} ions, respectively.

Since the excited CQDs transfer excitation energy to the proximal ground state RhB molecules through long-range dipole-dipole interactions based on FRET mechanism,[1,3] the FL emission of CQDs reduces with the increase of FL emission of RhB. Thus, the intensity ratio between the FL peaks at 581 nm (F_a) and 427 nm (F_d) should reflect FRET efficiency at the same concentrations of CQDs and RhB in the system of RhB@CQDs.

Figure 4A shows the effects of pH values on the ratio of F_a/F_d. The values of F_a/F_d reach to the maximum and are kept almost unchanged at pH=6-8, suggesting higher FRET efficiency in around neutral environment. The pH value can modulate the electrostatic interaction between the CQDs and RhB molecules. As a consequence, the pH variation could influence the absorption ability between CQDs and RhB, which mainly relies on electrostatic reaction, and thus change the distance between them. This could result in the change of FRET efficiency on the basis of FRET mechanism. Figure 4B and C show the effects of the concentrations of CQDs and RhB on FRET efficiency. It can be seen that there is not a linear increase with the concentrations of CQDs and RhB. The optimal concentrations of CQDs and RhB are 0.559 mg mL^{-1} and 1.25 μM, respectively. Under such condition of the optimal concentrations of CQDs and RhB, the effects of pH values on the quenching rates of emission peak at 581 nm from RhB@CQDs in the presence of 500 μM Fe^{3+} ions are given in Figure 4D. The largest quenching rate can be obtained at pH=6.2.

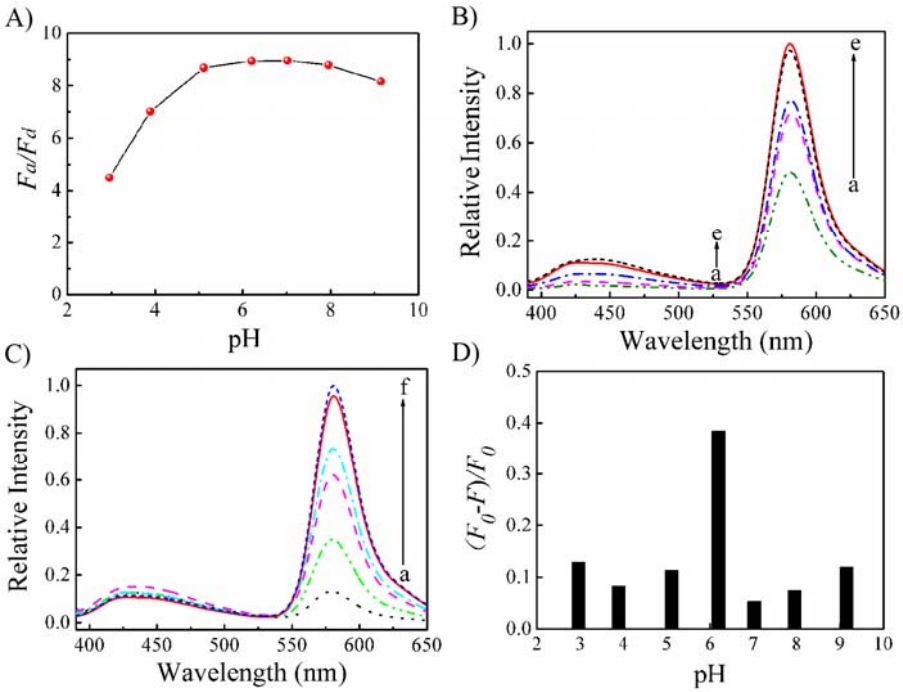

Figure 4 A) The effects of pH values on FRET efficiency of RhB@CQDs, where F_a and F_b are the intensities of FL emission peaks at 581 and 427 nm, respectively. B) The effects of the concentrations of CQDs on FRET efficiency of RhB@CQDs. Herein, the concentration increase of CQDs ranges from *a* to *e* (*a*–*e*: 0.14, 0.279, 0.419, 0.559, 0.698 mg mL^{-1}), RhB=1.25 μM, pH=6.20; C) The effects of the RhB concentrations on FRET of RhB@CQDs. Herein, the concentration increase of RhB ranges from *a* to *f* (*a*–*f*: 0.25, 0.5, 0.75, 1, 1.25, 1.5 μM), CQDs=0.559 mg mL^{-1}; pH=6.20; D) The relationship between FL emission quenching rates of RhB@CQDs in the presence of 500 μM iron ions and pH values under the condition of CQDs=0.559 mg mL^{-1} and RhB=1.25 μM, where F_0 and F are the FL emission intensities of RhB@CQDs at 581 nm without and with Fe^{3+} ions, respectively.

Fe^{3+} ions with varying concentrations were introduced to the system of RhB@CQDs that contained the optimal concentrations of CQDs and RhB at pH=6.2. Consequently, the emission peak at 581 nm was gradually quenched with the increase of Fe^{3+} ion concentrations (Figure 5A). The plot of emission intensity versus Fe^{3+} ion concentrations shows a linear relationship in a wide range with the correlation equation of F_0/F=1.0939+0.00911**C* (Fe^{3+}) (Figure 5B). The limit of Fe^{3+} ions, based on 3σ/ slope, was estimated to be about 30 nM.

The selectivity of RhB@CQDs towards Fe^{3+} was also evaluated according to the effects of tens of cations, including Fe^{3+}, Zn^{2+}, Pb^{2+}, Ni^{2+}, Na^{+}, Mn^{2+}, Mg^{2+}, K^{+}, Hg^{2+}, Fe^{2+}, Ca^{2+},

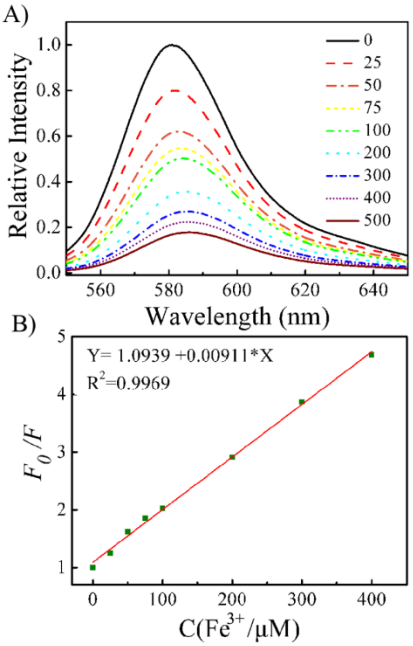

Figure 5 A) The FL emission spectra changes of RhB@CQDs with Fe^{3+} concentrations, *C* (from top to bottom: 0, 25, 50, 75, 100, 200, 300, 400 and 500 μM); B) The plot of F_0 /*F* against the concentrations of Fe^{3+},*C* under the conditions of CQDs=0.559 mg mL^{-1}, RhB=1.25 μM, pH=6.20.

Cu^{2+}, Cd^{2+}, Ba^{2+} and Al^{3+}, etc, on the emission response of RhB@CQDs as shown in Figure 6. Almost all of metal ions had no effects on emission peak at 581 nm of RhB@CQDs, except that Fe^{2+} could quench slightly this emission. It is noted that the higher quenching rate can be only obtained from the system of RhB@CQDs even though the emission of CQDs and RhB molecules can be also quenched by Fe^{3+} cations (Figure 6). Therefore, the RhB@CQDs sensor exhibited better performance than only CQDs or RhB molecules as the sensor in the detection of Fe^{3+} ions.

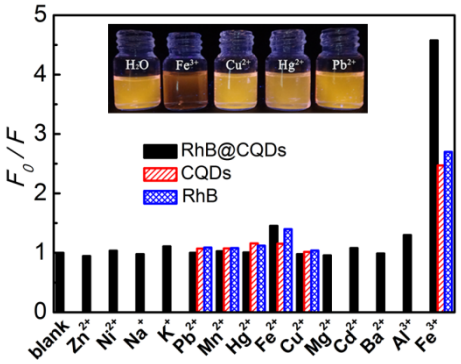

Figure 6 Histograms of F_0/F value, where F_0 and *F* are the FL emission intensities of RhB@CQDs (black), CQDs (red) and RhB molecules (blue) in the absence and presence of different metal ions of 500 μM, respectively, at the excitation wavelength of 365 nm. The inset is the photos of RhB@CQDs solutions (CQDs=0.559 mg mL^{-1}, RhB=1.25 μM, pH=6.20) without metal ions (H_2O) and with.

On the other hand, dozens of interfering cations with unknown concentrations but with known Fe^{3+} concentration were added into the detection system in order to further observe selectivity of RhB@CQDs towards to Fe^{3+} ions in the practical conditions. Results showed that the actual Fe^{3+} ions added and the Fe^{3+} value obtained from the above correlation equation had error range only 3-5%.

4. Discussion

According to the FRET principle, initially the donor CQDs absorbed the energy of the incident light and then transferred the excited state energy directly to the nearby acceptor RhB molecules without emitting the photons (Figure 7A). The energy transfer resulted in the decrease or quenching of the fluorescence of CQDs accompanied also by the enhancement in RhB fluorescence intensity. In addition to the overlapping emission and absorption spectra of CQDs and RhB molecules, FRET could occur between CQDs and RhB molecules that were separated by distances considerably larger than the sum of their van der Waals radii (1-10 nm)[31] and was governed by the Förster mechanism. According to the Förster model,[28] FRET efficiency (*E*) can be defined as

$$E = \frac{nR_0^6}{nR_0^6 + r^6} \quad (1)$$

where *r* is the separated distance between CQDs and RhB, *n* is the average number of RhB molecules interacting with one carbon quantum dot, R_0 is the Förster radius and expressed as[28]

$$R_0 = \left(\frac{6000(\ln 10) Q_D}{128 N_A \pi^5 n_D^4} I \right)^{1/6} \quad (2)$$

where N_A, Q_D and n_D are Avogadro's number, the quantum yield of CQDs, and the refractive index of the medium, respectively. *I* is the spectral overlap integral. The quantum yield of CQDs (Q_D) is a constant at the given incident light. However, *n* and *I* depend on the concentration ratio between CQDs and RhB molecules, thus causing the changes of FRET efficiency. The optimal concentrations of CQDs and RhB molecules were provided in the above experimental results (Fig. 3B and C).

When Fe^{3+} ions were added the system of RhB@CQDs, they could be adsorbed on the surface groups of CQDs and RhB molecules through the Brownian movement. Accoriding to above characterizations, CQDs with graphitic structure contained various types of oxidized carbon groups at their surface. RhB also presents O or N-contained groups at its molecular structure. Such active groups could specially combine with paramagnetic Fe^{3+} ions other than other cations through coordinate or chelate interaction, which has been widely used for color reaction in traditional organic chemisitry.[32-34] Accordingly, the excitation energy of CQDs migrate their nearer Fe^{3+} ions preferentially rather than the further RhB molecules by FRET process (Figure 7B). Because Fe^{3+} ions have the propensity to deactivate the excited state electrons by relaxation,[32,33] they act as the quenching centers. Fe^{3+} ions diffuse in a random-walk manner. Those excited CQDs and RhB molecules near Fe^{3+} ions relax predominantly by direct energy migration; those more distant Fe^{3+} ions, however, must fist diffuse into the vicinity of CQDs and RhB molecules before relaxation occurs. On the basis of diffusion limited energy transfer, the rate of excitation density of

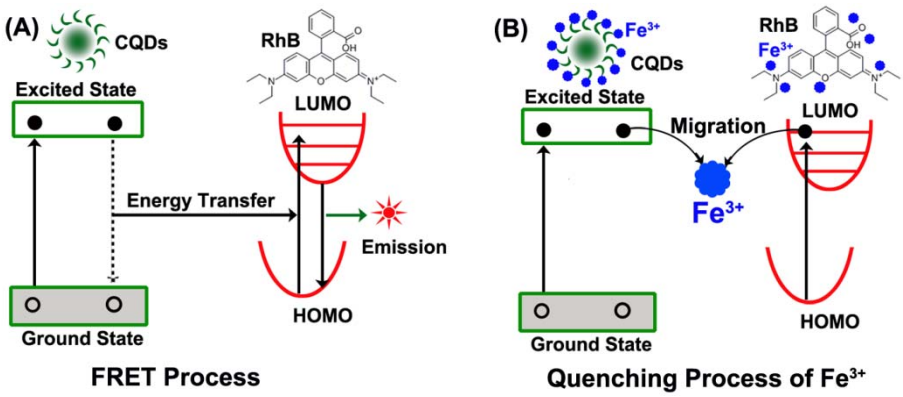

Figure 7 Schematic illustration of FRET process (A) and FL quenching mechanism of Fe^{3+} ions in RhB@CQDs (B). LUMO and HOMO represent the lowest unoccupied molecular orbital and highest occupied molecular orbital, respectively.

CQDs can be expressed as: [35]

$$\frac{\partial\phi(\vec{r},t)}{\partial t} = D\nabla^2\phi(\vec{r},t) - \sum\nu(\vec{r}-\vec{r}_n)\phi(\vec{r},t) - \frac{1}{\tau_0}\phi(\vec{r},t) \quad (3)$$

In equation (3), the fist item on the right represents the diffusion rate of Fe^{3+} ions where *D* is the diffusion constant; the second and third represent the probability of energy transfer, the intrinsic decay probability of CQDs, respectively.

When the concentration of Fe^{3+} ions is low, only a small fraction of the total number of excited CQDs and RhB molecules are within the critical migration distance of Fe^{3+} ions. In this limit, the principally excited state energy of CQDs can be still transferred into the nearby RhB molecules. As the concentration of Fe^{3+} ions is increased, a larger fraction of CQDs and RhB molecules are surrounded by Fe^{3+} ions and within the critical interaction range of energy migration. FRET process is completely limited and the intrinsic FL emission of RhB molecules is affected due to the migration of their excited state energy into Fe^{3+} ions. This accounts for Fe^{3+} concentration quenching of fluorescence emission from RhB@CQDs system.

5. Application

To investigate the potential use of this sensor, an attempt was made to monitor Fe^{3+} on the surface of the iron sheet and stainless steel in the process of metal corrosion. Iron and stainless steel sheets were polished with sandpaper until the surface of the metal was very smooth. Then they were washed with distilled water and ethanol several times, and dried in a vacuum oven at 60 ^{o}C for 2 h. RhB@CQDs were added into polyvinyl alcohol (PVA) aqueous solutions (5 %, w/v) that were prepared by dissolving PVA powders in deionized water and thereafter obtaining the RhB@CQDs-PVA sol that was employed to coat on the prepared Iron and stainless steel sheets.

Figure 8 shows the photos of RhB@CQDs-PVA films upon iron (Ⅰ) and stainless steel (Ⅱ) sheets under the visible light and UV lamp. It can be seen that the emission intensity of RhB@CQDs-PVA films upon iron sheets reduces with the time under the UV lamp. In contrast, neither this phenomenon takes places on the stainless steel sheet. The above results could be attributed to the differences of corrosion-resistant ability between iron and stainless steel at ambient conditions. Since these differences can be hardly distinguished by naked eyes, our proposed sensor of RhB@CQDs will be potential in application of fast monitoring the process of iron metal corrosion, helping us avoid sudden failure of devices and equipments.

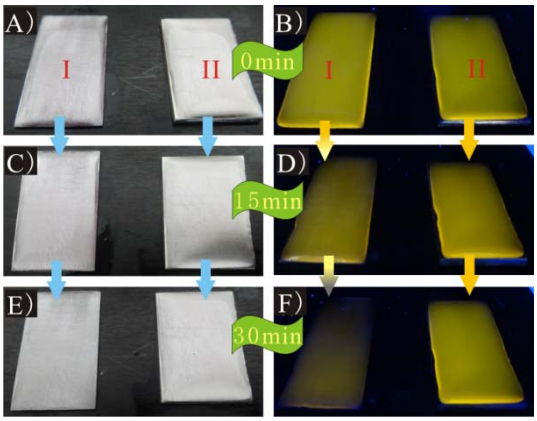

Figure 8 Photos of RhB@CQDs-PVA film upon iron (Ⅰ) and stainless steel (Ⅱ) sheets with time (0, 15 and 30 min) under the visible light (A, C, E) and UV lamp (B, D, F).

6. Conclusions

CQDs that could recognize Fe^{3+} ions were prepared by hydrothermal treatment of ethylene glycol and then they were mixed with RhB molecules. As the energy donor, CQDs can transfer the excited state energy into RhB acceptors to enhance FL emission of RhB molecules. Fe^{3+} ions can be adsorbed on the surface of CQDs and RhB molecules. The excited state energy from CQDs and RhB molecules are preferentially migrated into Fe^{3+} ions to relax, thus blocking FRET process and quenching of some intrinsic FL emission of RhB molecules. Accordingly, the sensor of RhB@CQDs combined the abilities of both CQDs and RhB towards Fe^{3+} detection. The higher sensitivity and selectivity were obtained. The RhB@CQDs sensor could be potential in application of fast monitoring corrosion process of iron devices and equipments.

Acknowledgments

We thank for financial support from the National Natural Science Foundation of China (Nos. 51272301, 51172214, 51172120), China Postdoctoral Science Foundation funded project (Nos. 2012M510788, 2013T60269), Shanxi Province Science Foundation for Youths (2014021008), 131 Talent Plan of Higher Learning Institutions of Shanxi, and State Key Laboratory of New Ceramic and Fine Processing Tsinghua University.

Notes and references

[a]*Key Laboratory of Instrumentation Science & Dynamic Measurement, Ministry of Education, Science and Technology on Electronic Test and Measurement Laboratory, Taiyuan 030051, P. R. China. *E-mail: hsliang@yeah.net* and *changneu@gmail.com ; Fax: +86 351 3559638; Tel.: +86 351 3559638*

[b]*School of Material Science and Engineering, North University of China, Taiyuan 030051, P. R. China*

[c]*State Key Laboratory of New Ceramics and Fine Processing, Tsinghua University, Beijing 100084, P. R. China*

‡*These authors contributed equally*

1 K. E. Sapsford, L. Berti, I. L. Medintz, *Angew. Chem. Int. Ed.,* 2006, **45**, 4562-4589.
2 C. R. Kagan, C. B. Murray, M. Nirmal, M. G. Bawendi, *Phy. Rev. Lett.,* 1996, **76**, 1517-1520.
3 J. S. Kim, D. T. Quang, *Chem. Rev.,* 2007, **107**, 3780- 3799.
4 A. Zheng, J. Chen, G. Wu, H. Wei, C. He, X. Kai, G. Wu, Y. Chen, *Microchim. Acta,* 2009, **164**, 17-27.
5 J. Li, F. Mei, W. -Y. Li, X. -W. He, Y. -K. Zhang, *Spectrochim.Acta.A:Mol. Biomol.Spectrosc.,*2008, **70**, 811-817.
6 A. Boulesbaa, Z. Huang, D. Wu, T. Lian, *J. Phys. Chem. C,* 2009, **114**, 962-969.
7 D. Gao, Z. Wang, B. Liu, L. Ni, M. Wu, Z. Zhang, *Anal. Chem.*,2008, **80**, 8545-8553.
8 B. Liu, F. Zeng, G. Wu, S. Wu, *Analyst,* 2012, **137**, 3717-3724.
9 X. Wang, X. Guo, *Analyst,* 2009, **134**, 1348-1354.
10 C. J. Murphy, *Anal. Chem.,* 2002, **74**, 520 -526.
11 H. Mattoussi, J. M.Mauro, E. R. Goldman, G. P. Anderson, V. C. Sundar, F. V. Mikulec, M. G.Bawendi, *J. Am. Chem. Soc.,* 2000, **122**, 12142- 12150.
12 W. C. Chan, D. J. Maxwell, X. Gao, R. E. Bailey, M. Han, S. Nie, *Curr. opin. biotechnol.,* 2002, **13**, 40-46.
13 X. Yan, X. Cui, B. Li, L. Li, *Nano Lett.*,2010, **10**, 1869-1873.
14 S. N. Baker, G. A. Baker, *Angew. Chem. Int. Ed.,* 2010, **49**, 6726-6744.
15 L. Zheng, Y. Chi, Y. Dong,J. Lin, B. Wang, *J. Am. Chem .Soc.,* 2009, **131**, 4564-4565.
16 R. Liu, D. Wu, S. Liu, K. Koynov, W. Knoll, Q. Li, *Angew. Chem. Int. Ed..,*2009, **121**, 4668-4671.
17 S. C. Ray, A. Saha, N. R. Jana, R. Sarkar, *J. Phys. Chem. C.,* 2009, **113**, 18546-18551.
18 H. Li, X. He, Y. Liu, H. Huang, S. Lian, S. -T. Lee, Z. Kang, *Carbon.,* 2011, **49**, 605-609.
19 A. B. Bourlinos, A. Stassinopoulos, D. Anglos, R. Zboril, M. Karakassides, E. P. Giannelis, *Small.*,2008, **4**, 455-458.
20 Y. Dong,R. Wang, G. Li, C. Chen, Y. Chi, G. Chen, *Anal. Chem.,* 2012, **84**, 6220-6224.
21 H. Li, J. Zhai, X. Sun, *Langmuir.,* 2011, **27**, 4305-4308.
22 H. Li, J. Zhai, J. Tian, Y. Luo, X. Sun, *Biosens.Bioelectron.*,2011, **26**, 4656-4660.
23 A. Zhu, Q. Qu, X. Shao, B. Kong, Y. Tian, *Angew. Chem .Int. Ed.,*2012, **51**, 7185-7189.
24 J. M. Liu, L. P. Lin, X. X. Wang,S. Q. Lin, W. L. Cai, L. H. Zhang, Z. Y. Zheng, *Analyst,* 2012, **137**, 2637-2642.
25 Y. Guo, Z. Wang, H. Shao, X. Jiang, *Carbon,* 2013, **52**, 583-589.
26 I. Vedrina-Dragojević, D. Dragojević, S. Čadež, *Anal. Chim. Acta.,* 1997, **355**, 151-156.
27 L. Balint, I. Vedrina-Dragojević, B. Šebečić, J. Momirović-Čuljat, M. Horvatić, *Microchimica Acta.,* 1997, **127**, 61-65.
28 A. R. Clapp, I. L. Medintz, J. M. Mauro, B. R. Fisher, M. G. Bawendi, H. Mattoussi, *J. Am. Chem. Soc.,* 2004, **126**, 301-310.
29 H. H. Cai, H. Wang, J. Wang , W. Wei, P. H. Yang, J. Cai, *Dyes Pigments,* 2012, **92**, 778-782.
30 S. Hu, R. Tian, Y. Dong, J. Yang, J. Liu, Q. Chang, *Nanoscale* 2013, **5**, 11665-11671
31 G. Chen, F. Song, X. Xiong, X. Peng, *Ind. Eng. Chem. Res.* 2013, **52**, 11228-11245
32 H. Huang, F. Liu, S. Chen, Q. Zhao, B. Liao, Y. Long, Y. Zeng, X. Xia, *Biosens. Bioelectron* 2013, **42**, 539-544
33 L. Fu, J. Mei, J. Zhang, Y. Liu, F. Jiang, *Luminescence* 2013, **28**, 602-606
34 D. Wang, L. Wang, X. Dong, Z. Shi, J. Jin, Carbon 2012, 50, 2147-2154
35 M. J. Weber, *Phys. Rev. B,* 1971, **4**, 2932-2939

